

LLM-Enhanced Multi-Agent Reinforcement Learning with Expert Workflow for Real-Time P2P Energy Trading

Chengwei Lou, Zekai Jin, Wei Tang, Guangfei Geng, Jin Yang, *Senior Member, IEEE*, Lu Zhang, *Senior Member, IEEE*

Abstract—Real-time peer-to-peer (P2P) electricity markets dynamically adapt to fluctuations in renewable energy and variations in demand, maximizing economic benefits through instantaneous price responses while enhancing grid flexibility. However, scaling expert guidance for massive personalized prosumers poses critical challenges, including diverse decision-making demands and lack of customized modeling frameworks. This paper proposed an integrated large language model-multi-agent reinforcement learning (LLM-MARL) framework for real-time P2P energy trading to address challenges such as the limited technical capability of prosumers, the lack of expert experience, and security issues of distribution networks. LLMs are introduced as experts to generate personalized strategy, guiding MARL under the centralized training with decentralized execution (CTDE) paradigm through imitation learning. A differential attention-based critic network is designed to enhance convergence performance. Experimental results demonstrate that LLM generated strategies effectively substitute human experts. The proposed multi-agent imitation learning algorithms achieve significantly lower economic costs and voltage violation rates on test sets compared to baselines algorithms, while maintaining robust stability. This work provides an effective solution for real-time P2P electricity market decision-making by bridging expert knowledge with agent learning.

Index Terms—P2P Energy Trading, Large Language Model, Multi-Agent Reinforcement Learning, Imitation Learning, Attention Mechanism

I. INTRODUCTION

THE rise of peer-to-peer (P2P) energy trading has shifted electricity users from traditional consumers to “prosumers,” combining both production and consumption [1]. However, this development faces two challenges: on the virtual layer, prosumers often lack the technical capability for repeated trading and efficient energy management [2]; on the physical level, ensuring system security during the transmission of electricity transactions from the virtual layer in actual distribution networks remains a challenge [3]. Additionally, traditional model-driven approaches fail to meet the dynamic response requirements of real-time P2P trading, resulting in a conflict between computational efficiency and

decision-making flexibility [4]. Thus, reinforcement learning (RL) has become a promising solution.

RL, due to its dependence on environmental interactions, faces challenges due to slow convergence and difficulty of reaching a global optimal solution [5]. Additionally, poor decision-making in the early training stages can endanger the security of the power grid. In response to these issues, mixed-integer programming-based expert solvers and imitation learning methods have improved the training efficiency of microgrid operation [6] and distribution network reconfiguration [7]. However, the decision-making driven by a single expert’s experience has limitations in adapting to the personality of prosumers in the P2P energy trading, as standardized strategies struggle to meet their diverse needs. Moreover, relying on a human Distribution System Operator (DSO) as the decision-making entity not only encounters practical limitations such as high labor costs and low response efficiency, but its inherent lack of generalization further exacerbates operational risks [8].

With the emergence of large language models (LLMs) like ChatGPT, LLMs showcase strong reasoning, decision-making, and generalization abilities, addressing the shortcomings of using single experts in RL to handle the heterogeneity of prosumers, as well as the challenges of human expert labor costs and generalization. While LLMs have begun to be applied in the power and energy sector—such as in [9], where LLMs replace humans for designing penalty functions in safe RL, [10] evaluates LLMs’ performance in various power system tasks, highlighting their potential in complex system modeling and reasoning. The study in [11] introduces a power multi-agent framework with a feedback mechanism, validated on the DALINE and MATPOWER platforms. However, the integration of LLMs as expert systems for assisting prosumers in RL training for P2P energy trading remains underexplored. Currently, in non-power system domains LLMs have been successfully used as expert guides in autonomous driving RL training [12], [13], providing valuable insights for the application of LLMs in the P2P energy trading domain.

Multi-agent Reinforcement Learning (MARL) stands out among RL approaches for P2P energy trading due to its capability to model strategic interactions among distributed prosumers in continuous action spaces, enabling decentralized decision-making and fostering collaborative behaviors. However, the complexity of managing numerous agents with high-dimensional actions under the Centralized Training and Decentralized Execution (CTDE) framework [14] limits the

This work was supported by Smart Grid-National Science and Technology Major Project(2024ZD0800500). (Corresponding authors: Zekai Jin; Lu Zhang). Chengwei Lou, Zekai Jin, Wei Tang, and Lu Zhang are with the College of Information and Electrical Engineering, China Agricultural University, Beijing, China. Guangfei Geng is with the School of Information Science and Technology, Guangdong University of Foreign Studies, Guangzhou, China. Jin Yang is with the James Watt School of Engineering, University of Glasgow, Glasgow, United Kingdom.

ability to exploit global collaborative information [15]. To improve learning efficiency, attention mechanisms have been introduced into MARL models [16] to better extract relevant features. Empirical studies confirm their effectiveness in power system applications such as voltage regulation [17], microgrid trading [18], and community-based P2P trading [19]. Nevertheless, conventional attention mechanisms often lack a holistic understanding of the entire sequence and may ignore critical information [20], which constrains MARL's performance in real-world P2P trading—an issue this work seeks to address.

In summary, this paper proposes an innovative integration framework that guides MARL training through LLM experts within the context of maximizing social welfare in local P2P real-time electricity markets involving prosumer collaboration. At the initial stage of training, the LLM generates model code based on differentiated prosumers' demands. Each prosumer's expert is embedded within a multi-LLM workflow, where real-time states are passed through to commercial solvers, indirectly generating expert strategies for each prosumer.

During the training phase, a CTDE-based MARL imitation learning algorithm is proposed. Moreover, inspired by the recent application of Differential Transformer in LLMs [21], we design an enhanced critic network architecture based on the differential attention. This architecture is specifically developed to mitigate irrelevant information interference from other agents during training and improve the overall convergence performance of the algorithm. The main contributions of this article are listed as follows:

- 1) A novel LLM-MARL integrated framework is proposed for the real-time P2P electricity market. By introducing LLMs as expert in the P2P energy trading, the framework replaces human experts to guide MARL agents during training. This significantly reduces manual intervention costs and achieves a deep integration of expert knowledge and LLM-based reasoning.
- 2) An LLM expert workflow tailored to local P2P electricity markets is developed for each prosumer. The workflow includes model generation, tool retrieval, code generation, and code correction. By processing state information, it dynamically generates prosumer strategies that balance economic performance and distribution network security, thus providing reliable expert guidance during training.
- 3) A novel multi-agent imitation learning algorithm is proposed. It introduces the Wasserstein metric to measure the similarity between expert strategy and agent policy, enabling effective guidance from the LLM experts' workflow. Furthermore, a differential multi-head attention-based Critic network is designed to improve policy evaluation accuracy and accelerate the learning process, thereby boosting overall algorithmic performance.

This paper is structured as follows: Section 2 introduces the system model and decentralized partially observable Markov decision process (Dec-POMDP) formulation for P2P energy trading. Section 3 details the integration of LLM and MARL. Section 4 presents numerical study and result analysis. Section 5 concludes the paper with key findings.

II. PRELIMINARIES

A. Prosumer energy management and P2P Trading

Prosumers are modeled as independent energy units with conventional distributed generators (CDGs), renewable distributed generators (RDGs), battery energy storage systems (BESSs), and controllable loads (CLs). A 15-minute interval is adopted for optimization, aligning with real-time P2P electricity market practices.

CDG output is limited by physical and safety constraints, including ramp rate limits on power variation. RDGs, such as Photovoltaic (PV) and Wind Turbine (WT), adjust active and reactive power via inverter control. BESS regulates energy flow within power and State of Charge (SOC) limits to prevent overcharging or deep discharge. CLs offer demand-side flexibility, adjusting consumption based on load characteristics and user preferences.

$$P_{i,\min}^{CDG} \leq P_{i,t}^{CDG} \leq P_{i,\max}^{CDG} \quad (1)$$

$$|P_{i,t}^{CDG} - P_{i,t-1}^{CDG}| \leq R_{i,\max}^{CDG} \quad (2)$$

$$0 \leq P_{i,t}^{RDG} \leq P_{i,t,\max}^{RDG} \quad (3)$$

$$P_{i,t}^{RDG,2} + Q_{i,t}^{RDG,2} \leq S_{i,\max}^{RDG,2} \quad (4)$$

$$P_{i,\min}^{BESS} \leq P_{i,t}^{BESS} \leq P_{i,\max}^{BESS} \quad (5)$$

$$SOC_{i,\min}^{BESS} \leq SOC_{i,t}^{BESS} \leq SOC_{i,\max}^{BESS} \quad (6)$$

$$SOC_{i,t}^{BESS} = \begin{cases} SOC_{i,t-1}^{BESS} + P_{i,t}^{BESS}/\eta, & P_{i,t}^{BESS} < 0 \\ SOC_{i,t-1}^{BESS} + \eta P_{i,t}^{BESS}, & P_{i,t}^{BESS} \geq 0 \end{cases} \quad (7)$$

$$0 \leq P_{i,t}^{CL} \leq \alpha P_{i,t}^{Load} \quad (8)$$

where $P_{i,t}^{CDG}$ is the CDG output, bounded by $[P_{i,\min}^{CDG}, P_{i,\max}^{CDG}]$ with ramp limit $R_{i,\max}^{CDG}$; $P_{i,t}^{RDG}, Q_{i,t}^{RDG}$ is the active / reactive power of RDG, limited by its maximum active power $P_{i,t,\max}^{RDG}$ and apparent power rating $S_{i,\max}^{RDG}$; $P_{i,t}^{BESS}$ is the power of BESS bounded by $[P_{i,\min}^{BESS}, P_{i,\max}^{BESS}]$; $SOC_{i,t}^{BESS}$ obeys efficiency η and bounded by $[SOC_{i,\min}^{BESS}, SOC_{i,\max}^{BESS}]$; $P_{i,t}^{CL}$ is the controllable load up to fraction α of its demand.

Prosumers at different nodes engage in P2P energy trading to increase their revenue. Each prosumer must satisfy an internal power balance, ensuring that generation, consumption, and storage remain aligned.

$$P_{i,t}^{EX} = -P_{i,t}^{Grid} - P_{i,t}^{P2P} = P_{i,t}^{CDC} + P_{i,t}^{RDG} + P_{i,t}^{CL} - P_{i,t}^{Load} - P_{i,t}^{BESS} \quad (9)$$

$$Q_{i,t}^{EX} = Q_{i,t}^{RDG} - Q_{i,t}^{Load} \quad (10)$$

where $P_{i,t}^{P2P}$ is the P2P electricity trading; $P_{i,t}^{Grid}$ is the active power purchase and sale with the grid; $P_{i,t}^{Load}, Q_{i,t}^{Load}$ are the active and reactive loads of prosumer.

Power flow constraints in the distribution network guarantee the safe, stable, and efficient operation of the power system.

$$P_{i,t}^{EX} = V_{i,t} \sum_{j \in \mathcal{N}} V_{j,t} (G_{ij} \cos \theta_{ij,t} + B_{ij} \sin \theta_{ij,t}), \quad (11)$$

$$Q_{i,t}^{EX} = V_{i,t} \sum_{j \in \mathcal{N}} V_{j,t} (-B_{ij} \cos \theta_{ij,t} + G_{ij} \sin \theta_{ij,t}), \quad (12)$$

$$V_{min} \leq V_{i,t} \leq V_{max}, \quad (13)$$

where $V_{i,t}$ is the node voltage magnitude and bounded by $[V_{\min}, V_{\max}]$; G_{ij}, B_{ij} is the conductance and susceptance of branch ij ; θ_{ij} is the voltage phase angle difference.

The total operational cost for a single prosumer C_i^{Cost} consists of the power purchase or sale cost from the grid C_i^{Grid} , CDG operational costs C_i^{CDG} , BESS maintenance costs C_i^{BESS} , CL compensation costs C_i^{CL} , and P2P energy trading costs C_i^{P2P} .

$$C_i^{Cost} = C_i^{Grid} + C_i^{CDG} + C_i^{BESS} + C_i^{CL} + C_i^{P2P}. \quad (14)$$

Prosumers' electricity purchase and sale costs follow time-of-use pricing. CDG operational costs are modeled as quadratic functions of fuel consumption. BESS costs depend on charging and discharging power, while CL costs reflect user dissatisfaction from load reduction. P2P trading incurs additional trading costs.

$$C_i^{Grid} = \sum_t \begin{cases} \lambda_t^S P_{i,t}^{Grid}, P_{i,t}^{Grid} < 0 \\ \lambda_t^B P_{i,t}^{Grid}, P_{i,t}^{Grid} \geq 0 \end{cases} \quad (15)$$

$$C_i^{CDG} = \sum_t c^{CDG} P_{i,t}^{CDG,2} + b^{CDG} P_{i,t}^{CDG}, \quad (16)$$

$$C_i^{BESS} = \sum_t \gamma |P_{i,t}^{BESS}|, \quad (17)$$

$$C_i^{CL} = \sum_t \rho |P_{i,t}^{CL}|, \quad (18)$$

$$C_i^{P2P} = \sum_t \lambda^{DSO} |P_{i,t}^{P2P}| + \lambda_t^{P2P} P_{i,t}^{P2P}, \quad (19)$$

where λ_t^B, λ_t^S are the time-of-use electricity purchase and sales price for the grid; c^{CDG}, b^{CDG} are the quadratic and linear cost coefficients of CDG fuel cost; γ is the maintenance cost coefficient; ρ is the compensation cost coefficient; λ_t^{DSO} is the P2P compensate fees charged by DSO; λ_t^{P2P} is the real-time P2P price.

The real-time P2P trading price λ_t^{P2P} is set as a fixed proportion between the grid's time-of-use buying and selling prices [22]. It is expressed as:

$$\lambda_t^{P2P} = \lambda^{P2P} (\lambda_t^B - \lambda_t^S) + \lambda_t^S, \quad (20)$$

where $\lambda^{P2P} \in [0, 1]$ is a price coefficient that determines the fairness of the P2P market. This pricing scheme incentivizes local trading by offering sellers a higher price than grid export rates and buyers a lower price than grid retail rates.

This paper aims to maximize the social welfare of prosumers by assuming that each prosumer makes rational trading decisions and accepts a centrally coordinated P2P price determined by the DSO. Whenever a prosumer experiences a surplus or deficit of electricity, it first seeks to balance supply and demand through local P2P energy trading.

$$\sum_i \sum_t \lambda_t^{P2P} P_{i,t}^{P2P} = 0, \quad (21)$$

However, within P2P energy trading, the total revenue of prosumers is 0 [23].

B. Dec-POMDP for P2P Energy Trading

In P2P energy trading, the inherent uncertainty challenges traditional mathematical optimization methods in meeting the precision and real-time demands of prosumer optimization control. RL methods can address these limitations, enabling data-driven optimization decisions. This paper models the P2P trading problem for multiple prosumers in a distribution network as a Dec-POMDP, represented as an eight-tuple $\langle I, A, S, O, P, r, \pi, \gamma \rangle$, where S is the global state space, A is the joint action space, r is the global reward function based on state transitions P , O is the observation space, and γ is the discount factor. The model captures the features of information asymmetry and decentralized decision-making through partial observability and decentralized architecture.

- 1) Agent: Each prosumer participating in P2P energy trading at a node in the distribution network is considered an agent. The set of agents is defined as I .
- 2) Action A : The joint action space at time t is represented by $a_t = \{a_{i,t} | i \in I\}$, where $\forall a_t \in A$. The action space of each agent, $a_{i,t}$, consists of the actions of controllable devices within the prosumer.

$$a_{i,t} = \left[P_{i,t}^{CDG}, P_{i,t}^{RDG}, Q_{i,t}^{RDG}, P_{i,t}^{BESS}, P_{i,t}^{CL} \right]. \quad (22)$$

- 3) State S : The global state at time t , denoted as $s_t = \{s_{i,t} | i \in N\}$, for $\forall s_t \in N$, encompasses the operational conditions of all nodes in the distribution network. Specifically, $s_{i,t}$ includes the operational state of the prosumer, the distribution network's interaction state, and the previous action of the prosumer:

$$s_{i,t} = \left[t, \lambda_t^B, \lambda_t^S, P_{i,t,\max}^{RDG}, P_{i,t}^{Load}, Q_{i,t}^{Load}, P_{i,t-1}^{CDG}, SOC_{i,t-1}, P_{i,t-1}^{P2P}, V_{i,t-1} \right]. \quad (23)$$

- 4) Observation O : The joint observation at time t is represented by $o_t = \{o_{i,t} | i \in I\}$, for $\forall o_t \in I$. The observation of the i -th agent at time t is the state of the corresponding node, i.e., $o_{i,t} = s_{i,t}$.
- 5) State Transition Probability P : The state transition is described by the conditional probability distribution $P(s_{t+1} | s_t, a_t)$, which represents the probability of transitioning to the next time step. This transition process considers power flow distribution, load demand fluctuations, and renewable energy output uncertainty. The power flow distribution is driven by the actions a_t of the controlled devices.
- 6) Reward Function r : All prosumers aim to achieve social welfare maximization by avoiding distribution networks voltage violations and minimizing costs. To this end, a unified global reward function is shared among all agents:

$$r = r^{Cost} + r^{Pen}, \quad (24)$$

$$r^{Cost} = \delta \sum_I C_i^{Cost}, \quad (25)$$

$$r^{Pen} = a^{Pen} + c^{Pen} \max\left\{0, \left| V_{base} - V_{i,t} \right| - \frac{V_{max} - V_{min}}{2} \right\}, \quad (26)$$

where δ is the weight coefficient for operational costs, and r^{Pen} represents the penalty cost for voltage violations in the distribution network.

III. METHODOLOGY

This paper focuses on P2P energy trading in distribution networks and introduces a novel MARL framework constrained by expert strategies. The proposed framework adopts an off-policy RL paradigm to enable efficient online updates. In this approach, LLM serves as an expert, generating personalized strategies to guide prosumers in energy trading. Fundamentally, it constitutes a form of “phase-triggered code synthesis training” enabled by LLM. Specifically, at the onset of each training phase, the LLM synthesizes optimization code tailored to the current system configuration. During subsequent online learning iterations, this code is executed in a loop to produce state-dependent, personalized strategies for each prosumer agent. To ensure a principled integration of expert knowledge with agent learning, the MARL algorithm is enhanced using the Wasserstein metric, which promotes alignment between the LLM strategy and the learned agent policies. When prosumer devices are modified or newly added, the LLM regenerates the code to adapt to the updated environment. As a result, the trained agent is capable of executing energy trading tasks autonomously without further LLM intervention. The overall framework is illustrated in Figure 1.

A. LLM Expert Workflow

1) *Knowledge Enhancement Methods:* Knowledge injection enhance the capabilities of LLMs and help mitigate information hallucination when these models act as domain experts. The main knowledge enhancement approaches include Supervised Fine-Tuning (SFT) and Retrieval-Augmented Generation (RAG). Unlike SFT, which requires full parameter fine-tuning, RAG decouples the knowledge storage from the inference generation. It only requires maintaining an external knowledge base. This characteristic not only ensures the real-time model outputs but also improves the interpretability of the generated results through explicit knowledge tracing. Recent research from Microsoft has demonstrated that RAG outperforms SFT in integrating domain-specific knowledge into LLMs [24], making RAG the core knowledge enhancement framework in this paper.

In constructing the knowledge system for LLM-based expert systems, this paper creates a structured JSON-format external knowledge base. JSON’s inherent facilitation of data extraction and processing, relative to alternative formats, establishes a robust foundation for retrieving broader and more precise knowledge during search operations [25]. The knowledge

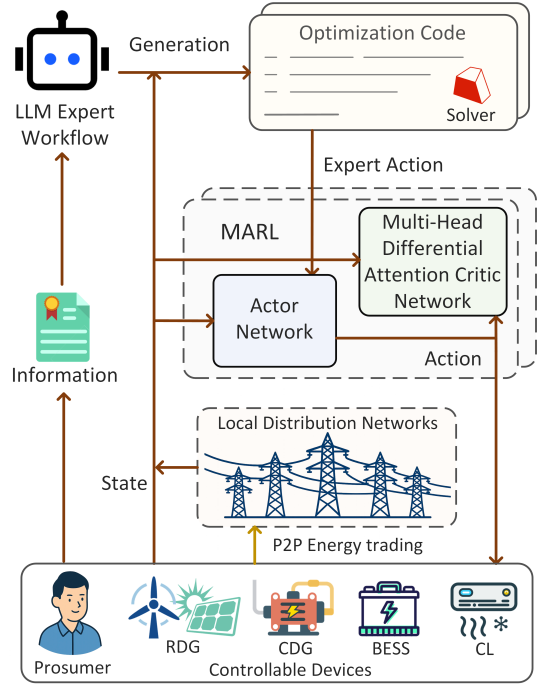


Fig. 1: Our proposed LLM-MARL framework

base integrates power domain expert knowledge and tool documentation, including system optimization models, devices, objective functions, constraints, and support for dynamic updates. Additionally, it includes detailed descriptions of the core classes, functions, and constraints in the cvxpy library [26]. Furthermore, this paper designs a multi-level prompt engineering strategy, which first clarifies the roles of various domain experts, then uses Chain-of-Thought techniques to guide experts in step-by-step reasoning, and ensures that the LLM structures content according to predefined rules.

2) *Prosumer-Centric LLM Expert Strategies:* This paper presents an LLM-based expert execution workflow to support personalized operational strategy for each prosumer. The system includes four complementary LLM agent expert and a module for distribution networks security verification via DSO. All optimization models are formulated in cvxpy and solved using commercial solvers such as Gurobi [27], CPLEX [28], or MOSEK [29]. The overall process is shown in the figure2, as described below:

- **Model Generation Expert:** This module LLM extracts key devices and optimization requirements from the input of the prosumer’s natural language, generates the corresponding model knowledge, and predicts relevant cvxpy Atoms and Constraints based on retrieval results and tool documentation.
- **Code Generation Expert:** This module LLM constructs the optimization model in the cvxpy framework using knowledge of the power domain, the cvxpy programming syntax, and the device parameters and state data of the prosumer. It outputs a DCP rules correct and feasible modeling code.
- **Iterative Correction Expert:** This module LLM runs the model in a sandbox environment using cvxpy together

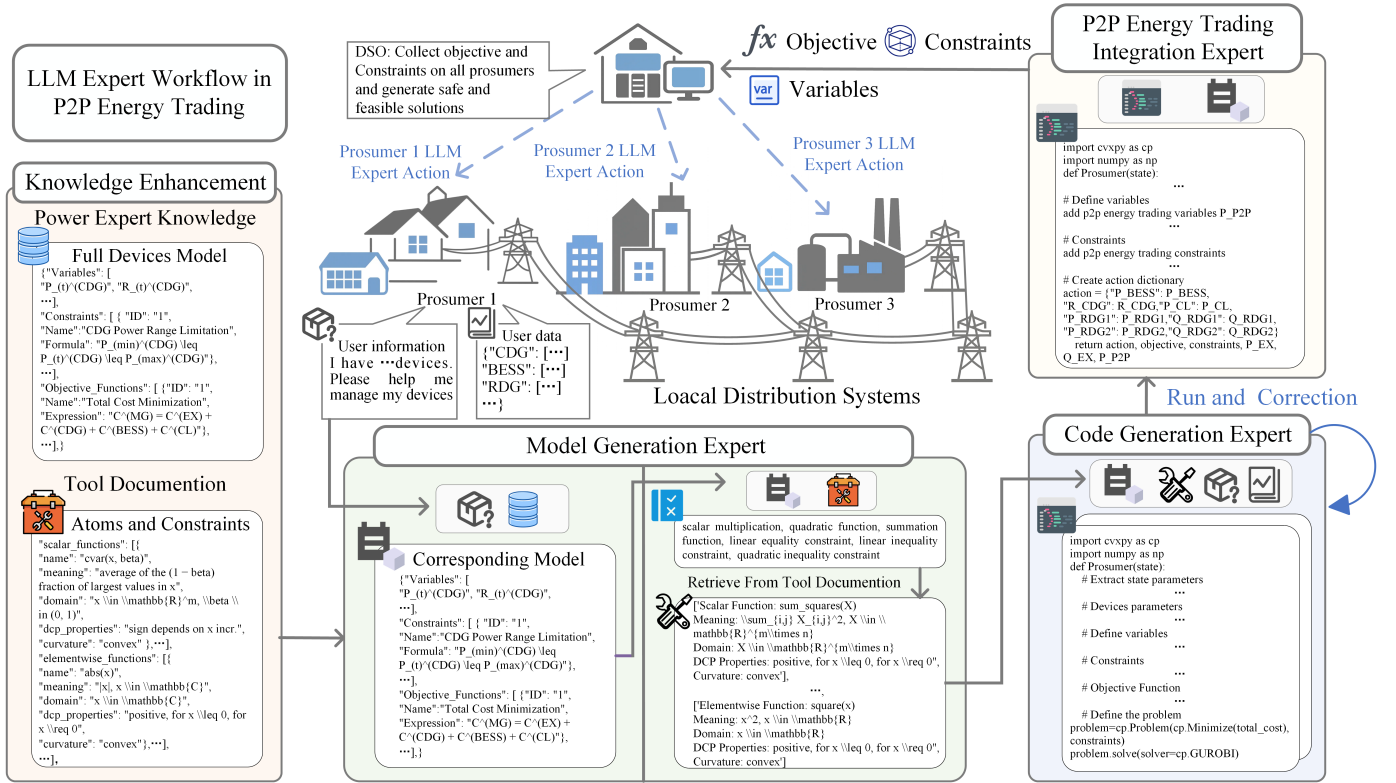


Fig. 2: Our proposed LLM expert workflow in P2P energy trading

with commercial solvers, detecting and correcting syntax errors and runtime issues, ensuring that the model is executable and complete.

- **Energy Trading Integration Expert:** After prosumer modeling and validation, this module LLM integrates the P2P energy trading variables into the optimization model, adding the necessary objective functions and constraints, and outputs personalized objective function, constraint list, and node injection of active and reactive power.
- **Distribution Networks Security Verification:** After all prosumer objectives and constraints are submitted, the DSO adds the objective functions and constraint sets of all prosumers. It then incorporates the active and reactive power node injections into the branch flow model [30] and invokes a commercial optimization solver to verify the global power flow correction across the distribution network, thereby generating optimized operating strategies for the prosumers.

B. Multi-Agent Imitation Learning Algorithm

For the prosumer collaborative learning problem, this paper proposes an expert strategy-constrained multi-agent imitation learning Algorithm based on the CTDE framework. The Algorithm constructs a joint state-action value function (Q-function) and state value function (V-function) through a centralized evaluation network, integrating the global environmental state and the behavior policies of all agents during the training phase, thereby guiding the differential optimization of individual agent policies. During execution, a decentralized

approach is adopted, where each agent independently makes decisions based on local observations through independently trained networks, balancing cooperative benefits and decision-making efficiency.

1) *Preparation:* The expert strategy constraints are embedded within a multi-agent actor-critic framework to solve the constrained optimization problem. Based on the Lagrangian dual theory, this problem is first transformed into its Lagrangian dual form. For each prosumer agent i , the multi-agent formulation is can be expressed as:

$$\begin{aligned} \min_{\pi} \mathbb{E}_{s_t \sim \mathcal{B}, a_t \sim \pi_{\phi_i}(\cdot | o_{i,t})} \left[- \min_{z \in \{1,2\}} Q_{\theta_{i,z}}(s_t, a_t) \right] \\ \text{s.t. } \hat{W}_2(\pi_{\phi_i}(\cdot | o_{i,t}), \pi^{LLM}(\cdot | o_{i,t})) \leq \epsilon, \end{aligned} \quad (27)$$

where \mathcal{B} is the experience replay buffer; ϕ is the actor network parameters and the output sampling from the Gaussian distribution $a_{i,t} \sim \mathcal{N}(\mu_{\phi_i}, \sigma_{\phi_i}^2)$; ϵ is the policy deviation; θ is the Q-function network parameters and $z = 1, 2$; ψ is the V-function network parameters. The policy network outputs a distribution over actions, which inherently facilitates exploration during training by enabling diverse action sampling under identical states.

Since the LLM-based expert strategies can only generate the mean parameters of the policy distribution, without estimating the standard deviation, the output is modeled as a Dirac delta function representing a degenerate distribution. To measure the similarity during policy iterations, the Wasserstein-2 metric, known for its distributional robustness, is used. In the case of a one-dimensional Gaussian distribution, \hat{W}_2^2 has a closed-

form analytical solution [31]:

$$\hat{W}_2^2(\pi_{\phi_i}(\cdot|o_{i,t}), \pi^{LLM}(\cdot|o_{i,t})) = \int_0^1 |F^{-1}(q) - G^{-1}(q)|^2 dq, \quad (28)$$

$$\int_0^1 (\mu_{\phi_i} + \sigma_{\phi_i} \Phi^{-1}(q) - a_{i,t}^{LLM})^2 dq = \int_0^1 [(\mu_{\phi_i} - a_{i,t}^{LLM})^2 + 2(\mu_{\phi_i} - a_{i,t}^{LLM})\sigma_{\phi_i} \Phi^{-1}(q) + \sigma_{\phi_i}^2 (\Phi^{-1}(q))^2] dq. \quad (29)$$

The resulting Wasserstein-2 metric between the expert strategy and the actor network is:

$$\hat{W}_2(\pi_{\phi_i}(\cdot|o_{i,t}), \pi^{LLM}(\cdot|o_{i,t})) = \sqrt{(\mu_{\phi_i} - a_{i,t}^{LLM})^2 + \sigma_{\phi_i}^2}. \quad (30)$$

2) *Multi-Head Differential Attention*: To enhance the modeling capability of the centralized critic in capturing inter-agent interactions, a multi-head differential attention mechanism is integrated into the critic network. This design aims to improve the accuracy of global value estimation. For each agent i , the input is first transformed into an embedding e_i and then concatenated into the resulting matrix E via an input embedding module, which is implemented as a multi-layer perceptron (MLP). Matrix E is then split into h attention heads and linearly projected into the query, key, and value spaces for each head, as follows:

$$[Q_1^h, Q_2^h] = EW^Q, [K_1^h, K_2^h] = EW^K, V^h = EW^V, \quad (31)$$

where $Q_1^h, Q_2^h, K_1^h, K_2^h, V^h \in \mathbb{R}^{d_{\text{model}}}$. The differential attention mechanism operates by subtracting two softmax-based attention maps, aiming to eliminate redundant information among agents and emphasize critical dependencies. The attention output for each head is computed as:

$$\text{head}^h = \left[\text{softmax}\left(\frac{Q_1^h K_1^{hT}}{\sqrt{d_k}}\right) - \xi^h \text{softmax}\left(\frac{Q_2^h K_2^{hT}}{\sqrt{d_k}}\right) \right] V^h, \quad (32)$$

$$X = \text{Concat}(\text{head}^1, \dots, \text{head}^h) W^O, \quad (33)$$

where W^O is a project matrix; scaling factor ξ^h is a learnable scalar and dynamically computed as:

$$\xi^h = \exp(\xi_{q_1} \cdot \xi_{k_1}) - \exp(\xi_{q_2} \cdot \xi_{k_2}) + \xi_{\text{init}}, \quad (34)$$

where $\xi_{q_1}, \xi_{q_2}, \xi_{k_1}, \xi_{k_2}$ are trainable vectors that vary with the head index.

To further enhance the representational capacity and mitigate issues such as gradient vanishing and feature degradation, a residual network structure is employed following the attention module. This design preserves input information and facilitates efficient training. The intermediate output X is then concatenated with the original input E and the combined vector is processed through another MLP to obtain the final output value. The architecture are shown in the figure 9.

The differential attention mechanism is motivated by the observation that, in real-time P2P energy trading, only a subset of prosumers significantly influences an agent's decision. For example, when an industrial prosumer exhibits high energy demand, cooperating with nearby prosumers possessing renewable surpluses can significantly enhance the social welfare. In

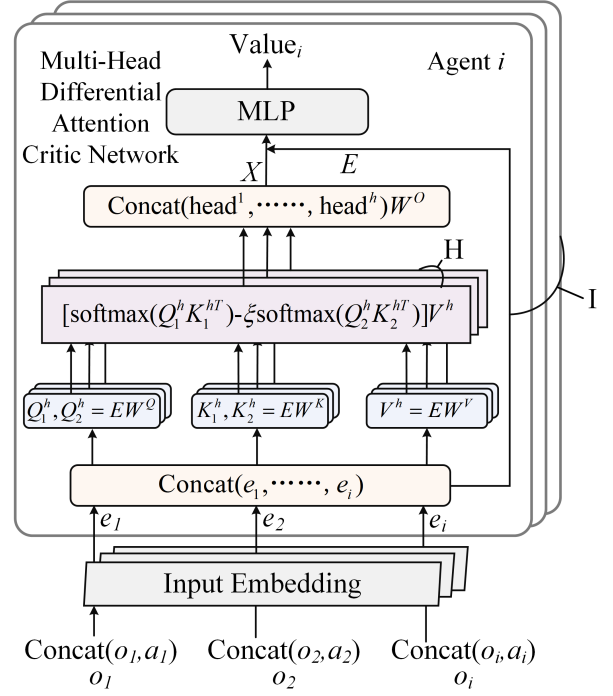


Fig. 3: Multi-head differential attention critic network

contrast, during low-demand periods, such trading interactions are less influential to the cooperative outcome. Conventional attention mechanisms may assign non-negligible weights to local irrelevant prosumers, thereby diluting focus on critical trading relationships. To address this, the proposed mechanism computes two attention maps, one capturing general relevance and the other suppressing redundant interactions, and subtracts them. This operation sharpens the critic network's focus on discriminative inter-agent dependencies, enabling more accurate value estimation.

3) *Learning the Critics*: In scenarios where agents share a global reward, a major challenge is to reduce the variance of policy gradient estimates in interactive multi-agent environments. To address this issue, a double Q-function network and a target V-function network are employed. The minimum selection operation in the double Q-function network effectively mitigates overestimation bias. The incorporation of a V-function network contributes to a significant reduction in estimation variance [32].

For V-function network V_{ψ_i} , which the loss function is calculated approximates the given the current state and Q-function values:

$$\mathcal{L}_V(\psi_i) = \mathbb{E}_{s_t \sim \mathcal{B}, a_t \sim \pi_{\phi_i}(\cdot|o_{i,t})} \left[(V_{\psi_i}(s_t) - \min_{z \in \{1,2\}} Q_{\theta_i,z}(s_t, a_t))^2 \right]. \quad (35)$$

For the Q-function network Q_{θ_i} , the training target y_t is computed using the a delay updated target network $V_{\bar{\psi}_i}$. The loss function is defined as follows:

$$\mathcal{L}_Q(\theta_i) = \mathbb{E}_{(s_t, \mathbf{a}_t, r_t, s_{t+1}) \sim \mathcal{B}} \left[\frac{1}{2} (Q_{\theta_i}(s_t, a_t) - y_t)^2 \right] \quad (36)$$

$$y_t = r_{i,t} + \gamma V_{\bar{\psi}_i}(s_{t+1}),$$

where the target V-function network $\bar{\psi}_i$ is updated via Polyak averaging rather than direct copying to enhance stability:

$$\bar{\psi}_i \leftarrow \tau \psi_i + (1 - \tau) \bar{\psi}_i, \quad (37)$$

where $\tau \ll 1$ is the smoothing coefficient.

4) *Learning the Actors*: Following the critic network update, the policy constraint in (27) can be expressed as a Lagrangian dual problem [33], where Lagrangian multipliers $\lambda_i > 0$. The formulation becomes:

$$\max_{\lambda} \min_{\pi} \mathbb{E}_{s_t \sim \mathcal{B}, a_t \sim \pi_{\phi_i}(\cdot | o_{i,t})} \left[- \min_{z \in \{1,2\}} Q_{\theta_{i,z}}(s_t, a_t) + \lambda_i \left(\hat{W}_2(\pi_{\phi}(\cdot | o_{i,t}), \pi^{LLM}(\cdot | o_{i,t})) - \epsilon \right) \right]. \quad (38)$$

Policy improvement serves to optimize and update the MARL policy. ϕ_i updated by minimizing the following loss function:

$$\mathcal{L}_{\pi}(\phi_i) = \mathbb{E}_{s_t \sim \mathcal{B}, a_t \sim \pi_{\phi_i}(\cdot | o_{i,t})} \left[- \min_{z \in \{1,2\}} Q_{\theta_{i,z}}(s_t, a_t) + \lambda_i \left(\hat{W}_2(\pi_{\phi}(\cdot | o_{i,t}), \pi^{LLM}(\cdot | o_{i,t})) - \epsilon \right) \right]. \quad (39)$$

By updating λ_i , the degree of constraint violation can be mitigated. This is achieved by minimizing the following loss function:

$$\mathcal{L}(\lambda_i) = \mathbb{E}_{s_t \sim \mathcal{B}} \left[- \lambda_i \left(\hat{W}_2(\pi(\cdot | o_{i,t}), \pi^{LLM}(\cdot | o_{i,t})) - \epsilon \right) \right]. \quad (40)$$

In the initial phase of training, a low policy deviation is employed to guide the agent’s learning; during the middle and later stages, a larger policy deviation is introduced to sustain the agent’s exploration. This framework ultimately enables efficient and stable policy optimization.

5) *Prioritized Experience Replay*: A sample loss-based priority evaluation mechanism is introduced. Samples with higher losses are considered more valuable for the learning process and are assigned higher priority, increasing their sampling probability.

Two experience replay buffers are defined: the normal operation experience replay buffer stores experiences collected during time steps where the agent’s actions do not cause voltage violations, reflecting typical operating conditions; the constraint violation experience replay buffer stores experiences from extreme renewable energy time steps in which the agent’s actions lead to grid voltage limit violations. During training, experiences are sampled from both buffers separately with a loss-based priority evaluation mechanism, drawn in a ratio of $k : (1 - k)$, to form training batches.

IV. NUMERICAL STUDY

To validate the effectiveness of the proposed framework, a numerical study is carried out on a modified IEEE 141-bus distribution networks, the voltage level is 12.47kV. As shown in Fig.4, 20 prosumers are selected to participate in local P2P energy trading, and the characteristics of five prosumer types are summarized in Table I. The renewable generation outputs and load demand curves of the prosumers are extracted from a real-world dataset published by the Belgian Transmission System Operator Elia [34].

Node	Devices Portfolio					Prosumer Scenario
	CDG	WT	PV	ESS	CL	
48,78,102,127,59,109,130,140	✓	–	✓	✓	✓	Commercial Rural
67,95,133,136	✓	✓	–	–	✓	Industrial
62,86,106,138	–	–	✓	✓	✓	Residential
74,100,116,134	✓	✓	✓	✓	✓	Energy Hub

TABLE I: Configurations of personalized prosumers

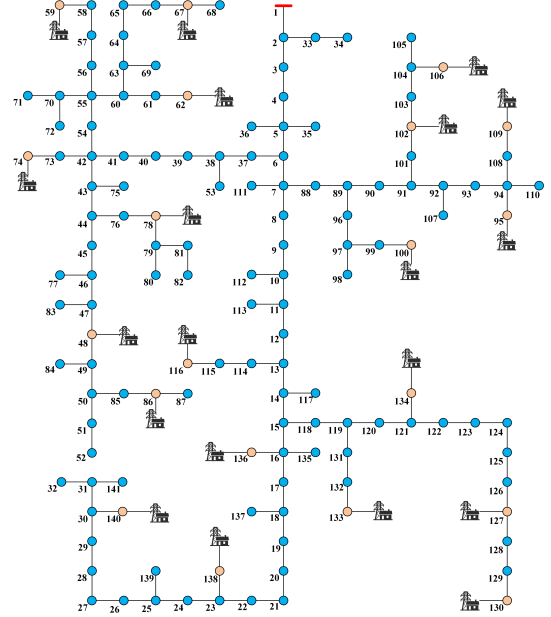


Fig. 4: IEEE141-bus distribution networks with twenty prosumers

A. Comparison Baselines

To evaluate the performance of the proposed algorithm, we compare it against the following baselines while also introducing:

- 1) MADDPG [35]: A CTDE-based multi-agent extension of DDPG employing a centralized critic and decentralized actors.
- 2) MAAC [36]: A CTDE framework augmented with a soft attention mechanism that adaptively weights and filters inter-agent information.
- 3) MATD3+BC [37]: Enhances MATD3 by incorporating a behavior-cloning loss to align each agent’s policy with LLM-generated expert actions.
- 4) MAGAIL [38]: A multi-agent adaptation of GAIL that uses an adversarial network to imitate expert trajectories provided by the LLM.
- 5) Our Proposed: Introduces a Lagrange multiplier during training to progressively constrain agent behaviors toward the LLM expert’s actions.
- 6) Our Proposed-MH: Extends the Our Proposed algorithm by integrating a differential multi-head attention mechanism into the critic to improve global value estimation.

B. Implementation Details

In terms of neural network architecture design, aside from

the variants incorporating attention mechanisms, all baseline algorithms share a unified network architecture under identical hyperparameter settings. The detailed hyperparameter settings are provided in TABLE II. Training was conducted for 5000 episodes with the same random seed initialization and update frequency. All experiments were implemented in Python 3.11.10 under the PyTorch 2.7, with parameters updated via the Adam optimizer. Computations were performed on a platform equipped with an NVIDIA RTX 5070Ti GPU, an AMD Ryzen ThreadRipper 3970X CPU, and 64GB of RAM.

TABLE II: HYPERPARAMETERS USED IN THE MARL

Symbol	Meaning	Value
lr	Learning rate	1e-4
$N_{episode}$	Maximum episode	5000
γ	Discount factor	0.99
N_B	Replay buffer size	1e5
B	Training batch size	128
λ	Initial Lagrange Multiplier	0.02
ϵ	Policy deviation	0.1
k	Proportion of normal replay buffer	0.8

Using year-round data, we designate the first day of each month as the validation set, the last week of each month as the test set, and the remaining days for training. A dynamic validation strategy is employed during training. After each training step, the current policy is evaluated using the validation set. The average cumulative discounted reward across all validation sets is recorded as the performance metric. To ensure statistical robustness, each algorithm is executed independently five times, and both the mean award and standard deviation of the resulting rewards are recorded.

In the present study, the LLM workflow is implemented through online API interfaces for experimental validation. Nevertheless, the proposed architecture is fully modular, allowing seamless substitution with locally hosted or SFT LLM instances to ensure data privacy and reduce latency. The LLM workflow is activated only during the training or system reconfiguration stages (e.g., when new devices are added or topology changes occur). During the training phase, each prosumer executes the LLM pre-generated optimization model code in parallel, while the DSO merely aggregates the objective functions and constraints from all prosumers and utilizes a commercial solver to generate secure operational strategies for each prosumer. In real-time operation, the lightweight MARL agents autonomously perform decision-making without further LLM guidance or global DSO validation. Consequently, the proposed framework achieves high computational efficiency and scalability, ensuring that decision-making comfortably satisfies the 15-minute market interval requirement even when extended to large-scale prosumer networks.

C. Performance Comparison

1) *Analysis of the LLM Expert Strategy:* In this evaluation, the human expert baseline refers to the optimal strategy obtained by solving a deterministic convex optimization model—formulated in accordance with the problem setting described in Section II—using the Gurobi commercial solver.

This model fully incorporates all physical constraints of the prosumers and minimizes the total operational cost under perfect forecasts of renewable generation and load demand. The resulting solver-based optimal policy serves as the ground-truth reference for assessing the accuracy of LLM-generated strategies.

Since the actions produced by the LLM expert directly influence subsequent MARL training, we evaluate the LLMs on the prosumer task using the following four key metrics:

- **Pass Rate:** The success rate of error-free, executable outputs, reflecting the LLM’s ability to generate valid code.
- **Accuracy:** For successful executions, accuracy quantifies the similarity to human expert actions based on cost deviation and action gap:

$$\text{Deviation} = \frac{|C^{\text{LLM}} - C^{\text{Human}}|}{C^{\text{Human}}} \times 100\%, \quad (41)$$

$$\text{Gap} = \frac{1}{T} \sum_{t=1}^T \left| \frac{a_t^{\text{LLM}} - a_t^{\text{Human}}}{a_t^{\text{Human}}} \right| \times 100\%, \quad (42)$$

$$\text{Accuracy} = 100\% - \frac{\text{Gap} + \text{Deviation}}{2}. \quad (43)$$

- **Correction:** The average number of code-fix iterations required before a successful execution, indicating generation efficiency.
- **Tokens:** The average number of completion tokens per successful run, reflecting the computational cost of generating expert policies.

The workflow is implemented using LangGraph [39], where the number of code generation iterations per execution cycle is capped at a maximum of 5 iterations. The temperature parameter is set to 0.5 to balance randomness and determinism in the model output. All experiments utilize the latest publicly accessible LLMs via official API interfaces. For each model, 10 experimental trials are conducted per type of prosumer request, resulting in 50 total trials per model. The detailed results are as follows:

TABLE III: Performance comparison of different LLMs in workflow

LLM	Pass Rate(%)	Accuracy (%)	Correction	Tokens
Chatgpt-4o	88	92.76	1.38	4727
Claude-3.5-Sonnet	94	99.41	0.95	5929
Gemini-2.5-Flash	92	98.65	1.24	18856
DeepSeek-V3	96	96.45	0.43	4039
Qwen-2.5-Max	90	99.62	1.54	5302
Chatgpt-o3	100	98.52	0.28	17195
Claude-4-Opus	100	99.93	0.20	9454
Gemini-2.5-pro	100	99.86	0.48	7558
DeepSeek-R1	100	98.31	0.54	16687
Qwen-3	100	99.84	0.33	8157

TABLE III provides a detailed comparison of the four metrics proposed in this study, where LLMs above the dashed line deactivate advanced reasoning capabilities, while those below activate it. The latency of a large model depends on network speed when API calls are used, but it is effectively eliminated when the model is deployed locally. Specifically, LLMs without advanced reasoning capabilities are generally more cost-efficient; among these, Google Gemini-2.5-Flash shows the highest average cost at 2.43 CNY (Derived from

the official billing statements of different LLMs after running the workflow once, and converted into CNY based on the prevailing exchange rate), mainly because it generates a larger number of output tokens per query, leading to higher overall billing despite its relatively low per-token price. In contrast, among reasoning-enabled models, Claude 4-Opus is the most expensive, with an average price of 6.27 CNY, primarily due to its higher per-token pricing structure reflecting the premium positioning of its advanced reasoning capabilities. Open-source LLMs such as DeepSeek and Qwen can further eliminate API-related expenses entirely when deployed locally.

The proposed multi-agent framework demonstrates superior model compatibility, enabling seamless integration with diverse mainstream LLMs rather than being constrained to the performance of a single model. A key finding is that the workflow exhibits exceptional performance on LLMs with advanced reasoning capabilities, achieving a 100% pass rate in the evaluated tasks; notably, Claude-4-Opus attains a level of proficiency that in these scenarios fully substitutes for human experts. The complete prompt–response records for the LLM evaluations are publicly accessible in the supplementary materials [40].

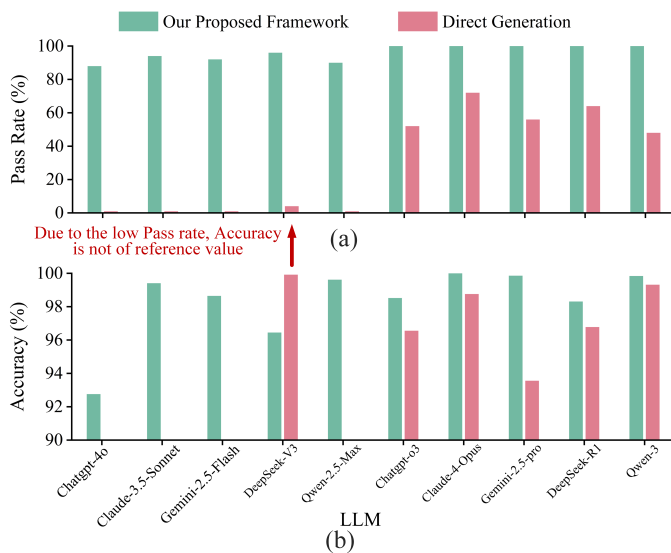


Fig. 5: Comparative experiments on the framework proposed in this paper

As demonstrated in Fig. 5, the results validate the effectiveness of the proposed LLM-expert workflow. Comparative experiments were conducted where LLMs could not access Atomic Function retrieval content. In this scenario, LLMs were required to generate code directly based on input models, data, and user information, and then perform power flow verification without any iterative code correction. Cross comparisons of two core metrics—Pass Rate and Accuracy—reveal that models without the integrated framework exhibit severe performance degradation. For deactivated advanced reasoning LLMs, pass rates approach zero due to primary failure modes such as “Model Infeasible or Unbounded” and “Numerical trouble encountered,” indicating significant gaps from human-expert-level performance.

The proposed LLM workflow demonstrates strong scalability within the scope of its structured knowledge base. Specifically, the LLM-based expert workflow can effectively accommodate different prosumer types, provided that the corresponding device models are already included in the knowledge base (note that constructing a comprehensive model repository is beyond the scope of this work, although research institutes, large utility companies and tech giants are already making efforts to build model libraries [41]). For each prosumer, the LLM dynamically generates personalized trading strategies based on its specific configuration. However, it is essential to recognize that when faced with requests involving device types or operational scenarios not covered by its knowledge base, the LLM may generate plausible but inaccurate or unsupported models or code, potentially compromising the accuracy and reliability of the resulting expert strategies.

2) *Performance Analysis of MARL Algorithm:* Claude-4-Opus is used as the expert LLM for algorithm performance comparison in this section. It uses three indicators: daily average reward, average operational cost, and average voltage violation rate to compare the proposed algorithm with the baseline algorithms:

The results in Fig. 6 demonstrate the performance of the proposed algorithm during training on the validation set. As shown, ‘Our proposed-MH’ achieves faster convergence to a low operational cost with minimal fluctuations, demonstrating enhanced reward stability for guiding agents when LLM outputs expert actions. Furthermore, the curve of average voltage violation rate for ‘Our proposed-MH’ rapidly declines and maintains a low level, highlighting its strength in constraint satisfaction and ability to maintain secure grid operations.

TABLE IV: Comparison of different algorithms on test set

Algorithm	Operational Cost (CNY)		Voltage Violation Rate (p.u)	
	Mean	Std. Dev.	Mean	Std. Dev.
MADDPG	6586.45	340.76	3.66×10^{-3}	8.47×10^{-4}
MAAC	5940.32	220.49	2.02×10^{-3}	7.29×10^{-4}
MATD3+BC	5489.20	207.88	1.61×10^{-3}	2.82×10^{-4}
MAGAIL	6380.96	164.23	2.82×10^{-3}	9.01×10^{-4}
OP	5146.27	146.07	1.39×10^{-3}	4.05×10^{-4}
OP-MH	4840.61	135.31	1.06×10^{-3}	3.03×10^{-4}

Note: OP stands for “Our Proposed.”

After completing model training, we applied the proposed algorithm to an test set to evaluate the practical applicability. As shown in TABLE IV, the proposed algorithm demonstrates significant advantages in both operational cost and voltage violation rate. Specifically, the average cost reached 4840.61 CNY, while the voltage violation rate was 1.06×10^{-3} . Through comprehensive analysis of mean-standard deviation comparisons with baseline algorithms, the proposed approach achieves optimal results across all three evaluation metrics. It maintains the lowest mean values while exhibiting minimal standard deviations, indicating not only superior average performance but also robust stability.

During the training process, the evolution of the agent average Lagrange multiplier λ and the average Wasserstein-2 metric provides key insight into the dynamic balance between expert imitation and autonomous policy optimization.

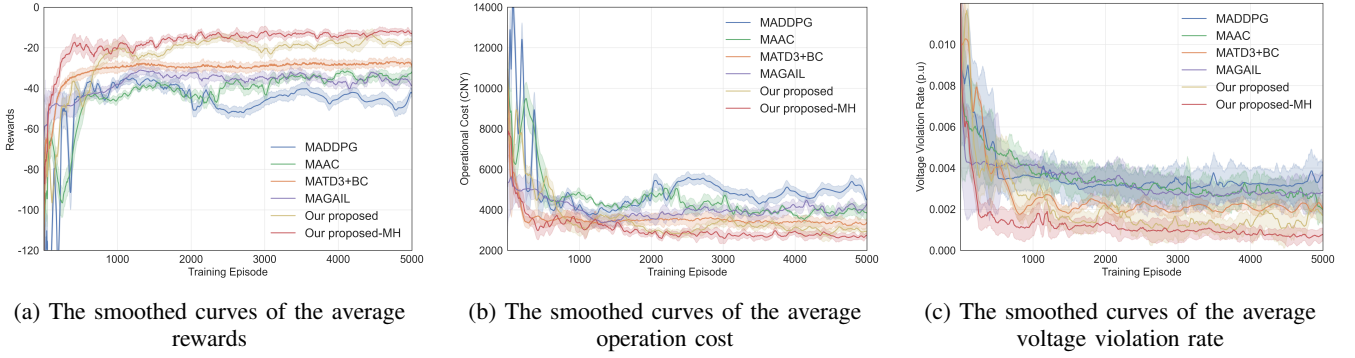


Fig. 6: Comparison chart of the performance of baseline algorithms

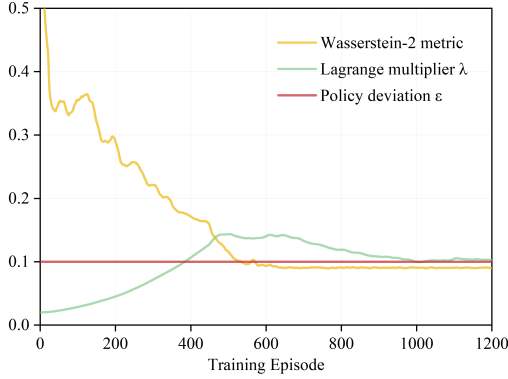


Fig. 7: Average Lagrange multiplier and Wasserstein metric during training episode

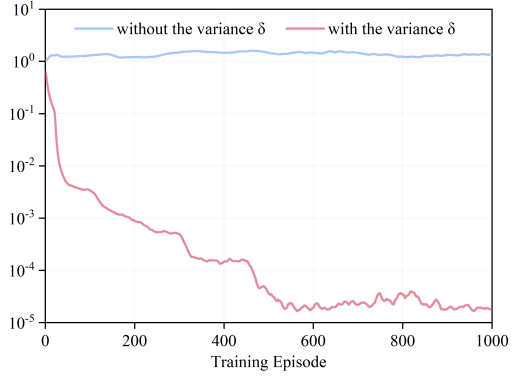


Fig. 8: Sensitivity analysis of Wasserstein metric variance term

As shown in Fig.7, λ initially increases rapidly, reflecting the strong constraint effect imposed by the LLM expert strategy to guide the early-stage exploration of the MARL agents. With the gradual improvement of policy learning, λ subsequently decreases and eventually stabilizes, indicating that the agents have progressively internalized the expert behavior and require less external constraint. In contrast, the Wasserstein-2 metric between the agent policy and the expert policy exhibits a consistently decreasing trend, demonstrating continuous convergence of the learned policy toward the expert distribution. Once the Wasserstein-2 metric approaches the predefined threshold Policy deviation ϵ , it remains stable, signifying that the imitation learning constraint has reached equilibrium and the training has achieved convergence.

To further investigate the sensitivity of the Wasserstein-based regularization, a comparative analysis was conducted between two formulations of the Wasserstein-2 metric in (30): one with the variance term σ and one without it. As illustrated in Fig.8, when the σ is incorporated, it converges smoothly to approximately 10^{-5} after around 500 episodes. This indicates that the stochastic exploration of the actor network is gradually reduced as the learned policy approaches the expert strategy, achieving a stable and deterministic behavior. In contrast, when the σ is excluded, the implied policy variance remains large and fluctuates around 1.2 throughout training, suggesting incomplete convergence, the agent's actions are not stable enough. These results highlight that explicitly learning and

regularizing the σ is crucial for maintaining exploration in the early stage while ensuring eventual convergence to a stable policy distribution.

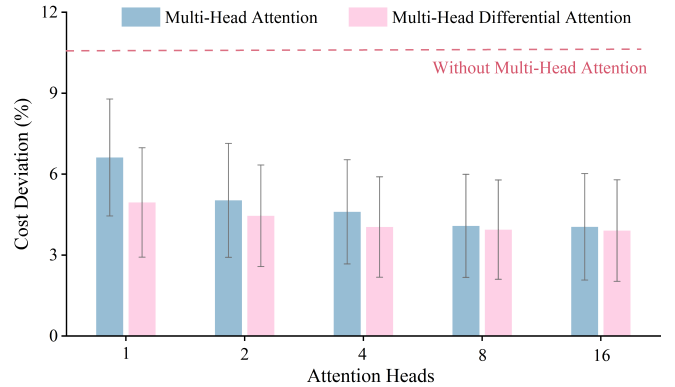


Fig. 9: Ablation study on the number of attention heads

To evaluate the effectiveness of the proposed differential attention mechanism in multi-agent P2P energy trading, ablation studies were conducted, with results shown in Fig. 9. Experimental findings reveal that the number of attention heads significantly impacts cost deviation in LLM expert. When the number of attention heads increases from a small value (e.g., from 0 to 1 or from 1 to 2), the system exhibits a significant reduction in cost deviation. This indicates that the introduction of a few attention heads provides substantial gains

in capturing key agent interactions. However, as the number of heads increases to a higher level (e.g., from 8 to 16), the performance improvement tends to saturate, and the reduction in cost deviation becomes marginal. This suggests that an excessive number of attention heads may introduce redundant information, thereby suppressing model performance. Furthermore, under the configuration where the head count satisfies $d_{model}/2d$, the differential attention mechanism demonstrates superior scheduling performance while maintaining equivalent parameter scale and computational complexity compared to standard attention mechanisms.

It is worth emphasizing that the precise optimization models generated by the LLM are only employed during the training phase, assuming access to future information, and therefore cannot be directly applied in real-world real-time P2P energy market environments. In our framework, the LLM functions solely as an expert sample generator in the training stage, which accelerates the convergence of MARL and mitigates the issues of slow convergence and high exploration cost inherent in reinforcement learning. After training is completed, the MARL policy network can make rapid decisions relying solely on the current state, thereby fully meeting the stringent timeliness requirements of real-time P2P energy markets.

It should be noted that, like most RL approaches, the proposed framework exhibits limited generalization capability and requires retraining [42] whenever the environment undergoes substantial changes, such as major topology re-configuration or the introduction of entirely new market mechanisms. Despite this inherent limitation of RL, the proposed LLM-MARL framework significantly outperforms conventional MARL methods in both convergence speed and final performance. To ensure reliability, all LLM generated strategies undergo DSO-based security verification, which guarantees their feasibility. Furthermore, the differential attention-based critic effectively mitigates performance degradation caused by increased agent interactions or system scale-up. As a result, the framework greatly reduces reliance on human expert guidance and significantly lowers the overall cost associated with full retraining in practical deployments.

V. CONCLUSION

This paper addresses the collaborative decision-making challenges among multiple prosumers in local real-time P2P electricity markets by proposing a framework that integrates LLM expert guidance with multi-agent imitation learning. This approach effectively overcomes limitations inherent in traditional optimization methods—particularly their inability to achieve real-time decision-making—as well as limitations of MARL without LLM guidance, particularly high manual labor costs associated with human expert involvement. The framework innovatively employs LLMs as expert to generate personalized strategies for guiding MARL training, combined with Wasserstein metric and an enhanced Critic network, achieving deep integration of expert knowledge and agent learning. This significantly reduces manual costs while enhancing policy optimization performance.

Experimental validation demonstrates the method's superior performance. In model compatibility tests, the proposed frame-

work exhibits universality across mainstream LLMs, with the Claude-4-Opus model achieving 100% pass rate and 99.93% accuracy in expert workflow task, effectively substituting human experts. In the modified IEEE 141-bus distribution network, the proposed method achieves a remarkably low average operational cost of 4840.61 CNY and a voltage violation rate of only 1.06×10^{-3} p.u., significantly outperforming conventional baseline methods.

Future work will extend to larger-scale prosumer groups, expand external expert knowledge repositories, and explore the adaptability of diverse LLM workflow architectures in complex scenarios to strengthen the framework's practical value.

REFERENCES

- [1] T. Capper, A. Gorbacheva, M. A. Mustafa, M. Bahloul, J. M. Schwidtal, R. Chitchyan, M. Andoni, V. Robu, M. Montakhabi, I. J. Scott, C. Francis, T. Mbavarira, J. M. Espana, and L. Kiesling, "Peer-to-peer, community self-consumption, and transactive energy: A systematic literature review of local energy market models," *Renewable and Sustainable Energy Reviews*, vol. 162, p. 112403, 2022.
- [2] C. Feng and A. L. Liu, "Peer-to-peer energy trading of solar and energy storage: A networked multiagent reinforcement learning approach," *Applied Energy*, vol. 383, p. 125283, 2025.
- [3] C. Feng, B. Liang, Z. Li, W. Liu, and F. Wen, "Peer-to-peer energy trading under network constraints based on generalized fast dual ascent," *IEEE Transactions on Smart Grid*, vol. 14, no. 2, pp. 1441–1453, 2023.
- [4] X. Xu, K. Xu, Z. Zeng, J. Tang, Y. He, G. Shi, and T. Zhang, "Collaborative optimization of multi-energy multi-microgrid system: A hierarchical trust-region multi-agent reinforcement learning approach," *Applied Energy*, vol. 375, p. 123923, 2024.
- [5] T. L. Paine, C. Gulcehre, B. Shahriari, M. Denil, M. Hoffman, H. Soyer, R. Tanburn, S. Kapturowski, N. Rabinowitz, D. Williams, G. Barth-Maron, Z. Wang, N. de Freitas, and W. Team, "Making efficient use of demonstrations to solve hard exploration problems," 2019. [Online]. Available: <https://arxiv.org/abs/1909.01387>
- [6] S. Gao, C. Xiang, M. Yu, K. T. Tan, and T. H. Lee, "Online optimal power scheduling of a microgrid via imitation learning," *IEEE Transactions on Smart Grid*, vol. 13, no. 2, pp. 861–876, 2022.
- [7] Y. Zhang, F. Qiu, T. Hong, Z. Wang, and F. Li, "Hybrid imitation learning for real-time service restoration in resilient distribution systems," *IEEE Transactions on Industrial Informatics*, vol. 18, no. 3, pp. 2089–2099, 2022.
- [8] C. Huang, Z. Tang, S. Hu, R. Jiang, X. Zheng, D. Ge, B. Wang, and Z. Wang, "Orlm: A customizable framework in training large models for automated optimization modeling," 2025. [Online]. Available: <https://arxiv.org/abs/2405.17743>
- [9] X. Yang, C. Lin, H. Liu, and W. Wu, "R12: Reinforce large language model to assist safe reinforcement learning for energy management of active distribution networks," *IEEE Transactions on Smart Grid*, vol. 16, no. 4, pp. 3419–3431, 2025.
- [10] C. Huang, S. Li, R. Liu, H. Wang, and Y. Chen, "Large foundation models for power systems," in *2024 IEEE Power & Energy Society General Meeting (PESGM)*, 2024, pp. 1–5.
- [11] M. Jia, Z. Cui, and G. Hug, "Enhancing llms for power system simulations: A feedback-driven multi-agent framework," 2025. [Online]. Available: <https://arxiv.org/abs/2411.16707>
- [12] C. Xu, J. Liu, S. Fang, Y. Cui, D. Chen, P. Hang, and J. Sun, "Tell-drive: Enhancing autonomous driving with teacher llm-guided deep reinforcement learning," 2025. [Online]. Available: <https://arxiv.org/abs/2502.01387>
- [13] H. Pang, Z. Wang, and G. Li, "Large language model guided deep reinforcement learning for decision making in autonomous driving," 2024. [Online]. Available: <https://arxiv.org/abs/2412.18511>
- [14] L. Kraemer and B. Banerjee, "Multi-agent reinforcement learning as a rehearsal for decentralized planning," *Neurocomputing*, vol. 190, pp. 82–94, 2016.
- [15] Y. Zhou, S. Liu, Y. Qing, K. Chen, T. Zheng, J. Song, and M. Song, "Is centralized training with decentralized execution framework centralized enough for marl?" 2025. [Online]. Available: <https://arxiv.org/abs/2305.17352>

- [16] Y. Wang, D. Shi, C. Xue, H. Jiang, G. Wang, and P. Gong, "Ahac: Actor hierarchical attention critic for multi-agent reinforcement learning," in *2020 IEEE International Conference on Systems, Man, and Cybernetics (SMC)*, 2020, pp. 3013–3020.
- [17] X. Yang, H. Liu, and W. Wu, "Attention-enhanced multi-agent reinforcement learning against observation perturbations for distributed volt-var control," *IEEE Transactions on Smart Grid*, vol. 15, no. 6, pp. 5761–5772, 2024.
- [18] F. Yang, D. Huang, D. Li, S. Lin, S. M. Muyeen, and H. Zhai, "Data-driven load frequency control based on multi-agent reinforcement learning with attention mechanism," *IEEE Transactions on Power Systems*, vol. 38, no. 6, pp. 5560–5569, 2023.
- [19] G. Gao, Y. Wen, and D. Tao, "Distributed energy trading and scheduling among microgrids via multiagent reinforcement learning," *IEEE Transactions on Neural Networks and Learning Systems*, vol. 34, no. 12, pp. 10 638–10 652, 2023.
- [20] S. Savino, T. Minella, Z. Nagy, and A. Capozzoli, "A scalable demand-side energy management control strategy for large residential districts based on an attention-driven multi-agent drl approach," *Applied Energy*, vol. 393, p. 125993, 2025.
- [21] T. Ye, L. Dong, Y. Xia, Y. Sun, Y. Zhu, G. Huang, and F. Wei, "Differential transformer," 2025. [Online]. Available: <https://arxiv.org/abs/2410.05258>
- [22] Y. Cui, Y. Xu, Y. Wang, Y. Zhao, H. Zhu, and D. Cheng, "Peer-to-peer energy trading with energy trading consistency in interconnected multi-energy microgrids: A multi-agent deep reinforcement learning approach," *INTERNATIONAL JOURNAL OF ELECTRICAL POWER & ENERGY SYSTEMS*, vol. 156, FEB 2024.
- [23] C. Mu, T. Ding, Y. Huang, S. Zhu, P. Siano, M. Shahidepour, and X. Shen, "Distributed collaboration method for peer-to-peer transactions in reconfigurable distribution network," *IEEE Transactions on Power Systems*, vol. 40, no. 4, pp. 3029–3042, 2025.
- [24] T. Xiao and P. Xu, "Exploring automated energy optimization with unstructured building data: A multi-agent based framework leveraging large language models," *Energy and Buildings*, vol. 322, p. 114691, 2024.
- [25] G. Dong, X. Li, Y. Zhang, and M. Deng, "Leveraging llm-assisted query understanding for live retrieval-augmented generation," 2025. [Online]. Available: <https://arxiv.org/abs/2506.21384>
- [26] S. Diamond and S. Boyd, "CVXPY: A Python-embedded modeling language for convex optimization," *Journal of Machine Learning Research*, vol. 17, no. 83, pp. 1–5, 2016.
- [27] *Gurobi Optimizer Reference Manual*, Gurobi Optimization, LLC, 2024. [Online]. Available: <https://www.gurobi.com>
- [28] *IBM ILOG CPLEX Optimization Studio CPLEX User's Manual*, IBM Corporation, 2024. [Online]. Available: <https://www.ibm.com/products/ilog-cplex-optimization-studio>
- [29] *The MOSEK Optimization Toolbox for MATLAB Manual*, MOSEK ApS, 2024. [Online]. Available: <https://www.mosek.com>
- [30] M. Farivar and S. H. Low, "Branch flow model: Relaxations and convexification-part i," *IEEE TRANSACTIONS ON POWER SYSTEMS*, vol. 28, no. 3, pp. 2554–2564, AUG 2013.
- [31] G. Peyré and M. Cuturi, "Computational optimal transport," *Foundations and Trends in Machine Learning*, vol. 11, no. 5-6, pp. 355–607, 2019.
- [32] X. Lyu, A. Baisero, Y. Xiao, and C. Amato, "A deeper understanding of state-based critics in multi-agent reinforcement learning," *Proceedings of the AAAI Conference on Artificial Intelligence*, vol. 36, no. 9, pp. 9396–9404, Jun. 2022. [Online]. Available: <https://ojs.aaai.org/index.php/AAAI/article/view/21171>
- [33] Z. Huang, J. Wu, and C. Lv, "Efficient deep reinforcement learning with imitative expert priors for autonomous driving," *IEEE Transactions on Neural Networks and Learning Systems*, vol. 34, no. 10, pp. 7391–7403, 2023.
- [34] Elia, "Elia wind/solar power/grid data set," <https://www.elia.be>, 2025, accessed: May 02, 2025.
- [35] M. Bettini, A. Prorok, and V. Moens, "Benchmarl: Benchmarking multi-agent reinforcement learning," 2024. [Online]. Available: <https://arxiv.org/abs/2312.01472>
- [36] S. Iqbal and F. Sha, "Actor-attention-critic for multi-agent reinforcement learning," 2019. [Online]. Available: <https://arxiv.org/abs/1810.02912>
- [37] S. Fujimoto and S. S. Gu, "A minimalist approach to offline reinforcement learning," 2021. [Online]. Available: <https://arxiv.org/abs/2106.06860>
- [38] J. Song, H. Ren, D. Sadigh, and S. Ermon, "Multi-agent generative adversarial imitation learning," 2018. [Online]. Available: <https://arxiv.org/abs/1807.09936>
- [39] LangChain Inc. LangGraph. [Online]. Available: <https://langchain-ai.github.io/langgraph/>
- [40] [Online]. Available: <https://github.com/jzk0806/P2P-llm-supplementary>
- [41] E. P. R. I. (EPRI), "Open power ai consortium," <https://msites.epri.com/opai>, 2025, accessed: 2025-10-21.
- [42] K. Cobbe, O. Klimov, C. Hesse, T. Kim, and J. Schulman, "Quantifying generalization in reinforcement learning," in *Proceedings of the 36th International Conference on Machine Learning*, ser. Proceedings of Machine Learning Research, K. Chaudhuri and R. Salakhutdinov, Eds., vol. 97. PMLR, 09–15 Jun 2019, pp. 1282–1289. [Online]. Available: <https://proceedings.mlr.press/v97/cobbe19a.html>